Bull Astr. Soc. India (1984) 12, 52-60

Mass transfer in AR Lacertae

R. K. Srivastava *Uttar Pradesh State Observatory, Manora Peak, Naini Tal 263 129*

Received 1983 November 2; accepted 1983 December 24

Abstract. Evolutionary discussion shows that the possibility of AR Lac being in a semi-detached state of evolution cannot be ruled out. The period variations of AR Lac have been analysed using Biermann & Hall's (1973) model for a system undergoing mass transfer. The yearly rates of period change and mass transfer are found to be respectively 1.7×10^{-6} d and $6.2 \times 10^{-7} M_{\odot}$.

Key words : period changes—mass transfer—RS CVn binaries

1. Introduction

The Algol system AR Lac (= BD + 45°3813 = HD 210334 = HV 2980) was found to be a variable by Miss Leavitt (1907), an eclipsing binary by Jacchia (1929) and Loreta (1929, 1930). Several authors attempted photometric, spectroscopic and radio observations of the system (cf. Wood *et al.* 1980). Recently, Kurutac, *et al.* (1981), Ertan *et al.* (1982) and Nha & Kang (1982) have presented two-colour photometry of AR Lac. Naftilan & Aikman (1981) and Kiziloğlu *et al.* (1983) have discussed spectroscopic observations of the system, which is a member of the RS CVn group (Hall 1976).

The geometrical elements of AR Lac obtained employing Russell & Merrill's (1952) method, absolute dimensions and Roche constants have already been reported (Srivastava 1981). The system has been reanalysed using Kopal's (1979) method, and revised geometrical elements, absolute dimensions, Roche constants for equipotential surfaces and Roche radii of the components have been determined (Srivastava 1983).

2. Evolutionary discussion

The values of the Roche constants, radii (r) and Roche radii (r^*) are :

$$C_0 = 4.0,\ C_1 = 7.5,\ C_2 = 4.3,\ C_2/C_0 = 1.08,$$

$$r_p = 0.17,\ r_p^* = 0.38,\ r_s = 0.34 \text{ and } r_s^* = 0.38,$$

where the subscripts p and s refer to the primary and secondary respectively. From the $\left[\log\left(\frac{M}{M_{\odot}}\right), \log\left(\frac{R}{R_{\odot}}\right)\right]$ plot (figure 1) and the [spectral type, M(bol)] plot (figure 2) (cf. Kopal 1955; Arp 1958), it is evident that the secondary component

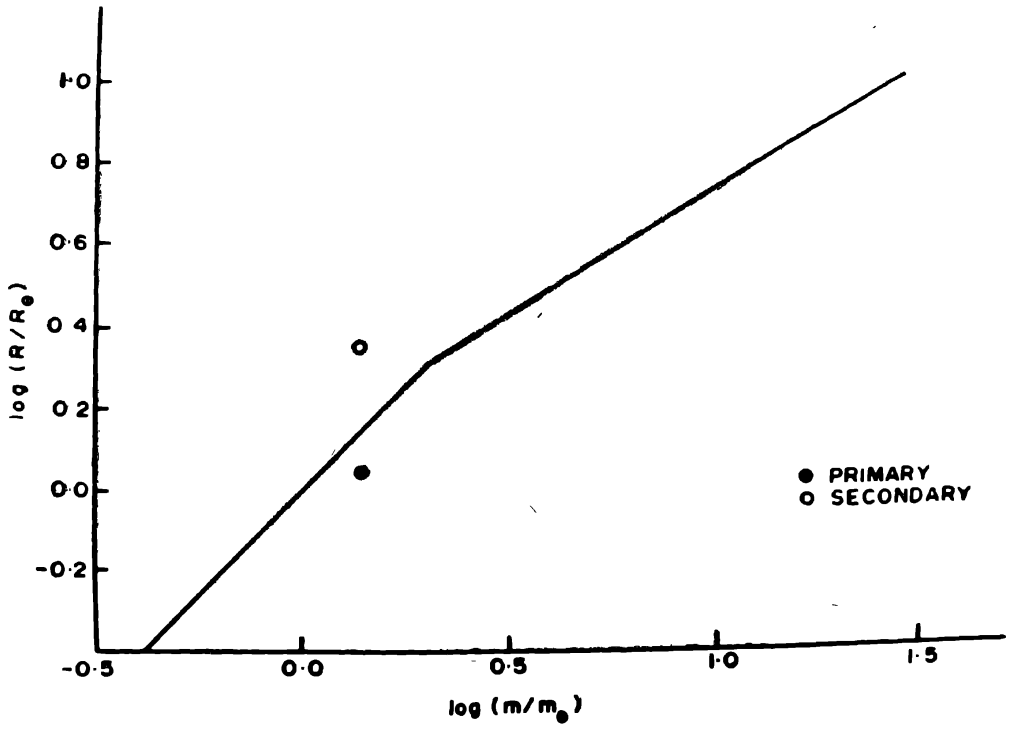

Figure 1. The position of the components of AR Lac on the mass-radius relation for close binary systems with detached components. The line on the diagram represents the average trend of the main-sequence.

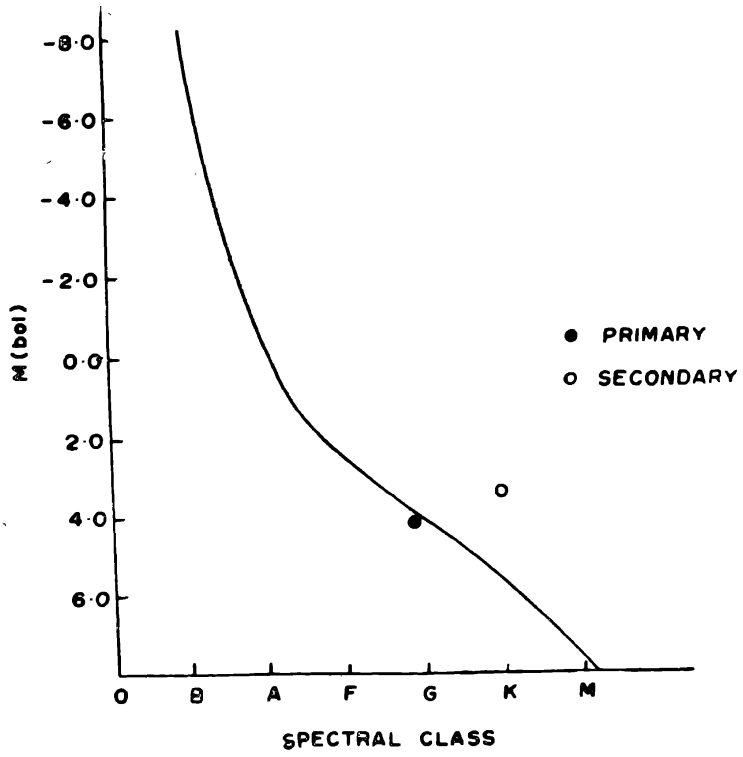

Figure 2. The position of the components of AR Lac on spectral class-luminosity relation for the main-sequence stars. The continuous line on the diagram schematizes the average trend of the main-sequence.

of AR Lac is away from the main-sequence, whereas the primary component lies nearly on the main-sequence.

The Roche constants show that $C_2/C_0 \simeq 1$. This fact suggests that AR Lac is in a semi-detached state of evolution, and may be possessing a subgiant secondary (Kopal 1959, p. 491). Since $r_s^* \simeq r_s$, the secondary component seems to have nearly filled its Roche lobe, and thus can be considered to be semidetached.

Schneller (1962) listed AR Lac as being between the detached and semidetached state of evolution. Kopal (1959, p. 491) explained that systems with sub-giants while being detached are nearly or actually in contact with the inside surface of the Roche lobe. Naftilan & Drake (1977) found that the metal abundances of AR Lac resemble those seen in Algol-type systems, which may suggest a similar evolutionary history for the RS CVn binaries.

The space distribution and velocity studies, the lack of nearby nebulosity, and the fact that the lithium has never been reported in these systems argue against a pre-main-sequence evolution of RS CVn binaries (Naftilan & Drake 1977). The post-main-sequence evolution appears to be more probable for the RS CVn binaries.

In conclusion, AR Lac appears to be in a semidetached state of evolution.

3. Period study

Besides the authors, given in table 1, many others have devoted their efforts for the observations of primary minimum and/or period studies of the system (Wood *et al.* 1980; Srivastava 1981). Recently such studies have been carried out by De Campli & Baliunas (1979), Hall & Kreiner (1980), Krutac *et al.* (1981), Ertan *et al.* (1982) and Nha & Kang (1982).

4. The O—C diagram, period variation and mass transfer

For studying the period variation we have calculated the $O - C$ values of available times of primary minima between 1900 and 1975 based on the ephemeris :

$$\text{Primary Minimum} = \text{JD } 2415300.059 + 1^d.983200.$$

The epoch is the oldest epoch by Dugan & Wright (1939) and the period is by Guarnieri *et al.* (1975). We have constructed an $O - C$ diagram by plotting the $O - C$ values against the cycles elapsed since the epoch given by Dugan & Wright (1939). The $O - C$ values are listed in table 1, and the $O - C$ diagram is shown in figure 3. An inspection of the diagram reveals that the time interval (1900 to1975) gets split up into four parts corresponding to the portions AB, BC, CD and DE of the diagram. The $O-C$ diagram suggests that there was a sudden period decrease around the years 1936 (around E = 6550) and 1967 (around E = 12525) and a period increase around 1947 (around E = 8650).

The extent of the period decrease and increase has been estimated in different portions of the $O - C$ diagram (figure 3) and the corresponding instant period at each of the points B, C, D and E calculated, assuming the instant period at point A to be $1^d.983200$. These are listed in table 2.

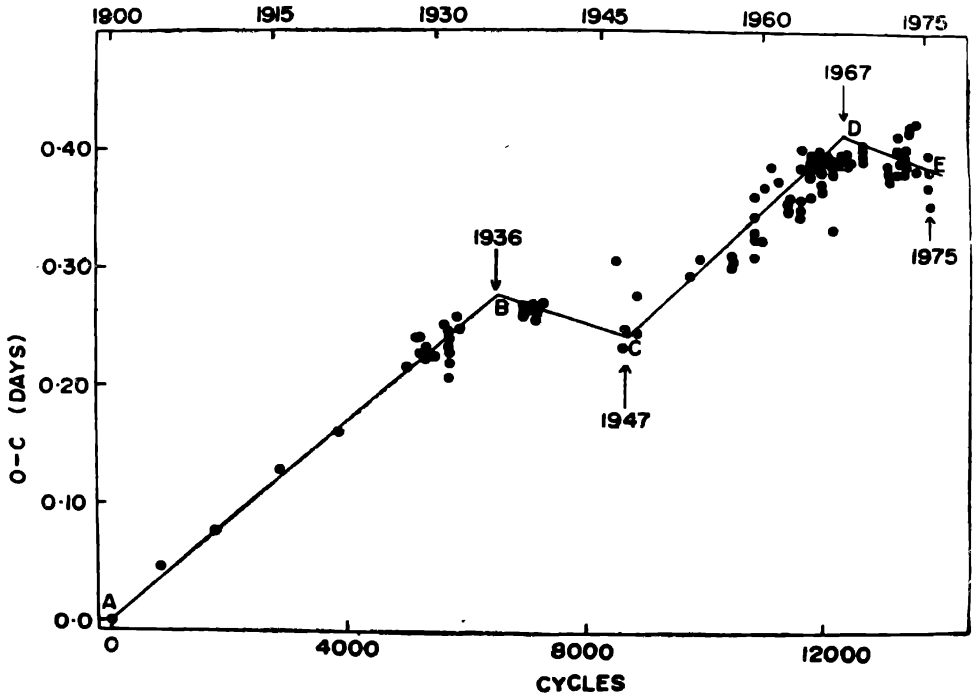

Figure 3. The $O-C$ diagram of AR Lac.

Table 1. Primary minima of AR Lac

Times of primay minima ($JD_{\odot}$)	Cycle	$O-C$	Reference
2415300.059	0	0^d.000	9
7005.649	860	+0.048	9
8889.729	1810	+0.078	9
2420991.973	2870	+0.130	9
2995.038	3880	+0.163	9
5196.444	4990	+0.217	9
5555 428	5171	+0.242	18
5573.278	5180	+0.243	26
5712.086	5250	+0.227	40
5801.328	5295	+0.225	31
5803.320	5296	+0.234	32
6146.405	5469	+0.225	38
6489.526	5642	+0.253	38
6592.651	5694	+0.251	38
6604.548	5700	+0.249	46
6622 395	5709	+0.247	38
6624.3314	5710	+0.200	13
6624.338	5710	+0.207	13
6624.378	5710	+0.247	38
6626.334	5711	+0.220	38
6626.361	5711	+0.247	38
6842.542	5820	+0.259	9
6991.286	2895	+0.263	14
9115.290	6966	+0.260	25
9150.992	6984	+0.264	43
9176.775	6997	+0.266	43
9178.760	6998	+0.267	43
9178.761	6998	+0.268	44
9182.725	7000	+0.266	43
9186.693	7002	+0.268	44
9188.675	7003	+0.266	44

Continued

Table 1—*Continued*

Times of primary minima ($JD_{\odot}$)	Cycle	$O-C$	Reference
9303.696	7061	+0^d.262	15
9404.847	7112	+0.270	44
9515.895	7168	+0.258	43
9523.832	7172	+0.263	43
9529.785	7175	+0.266	43
9535.739	7178	+0.270	44
9692.411	7257	+0.270	10
2432125.836	8484	+0.308	43
2476.789	8661	+0 235	43
2478.784	8662	+0.247	43
2843.690	8846	+0.244	43
2889 336	8869	+0.276	1
4235.918	9548	+0.255	15
4646.470	9755	+0.295	42
4888.429	9877	+0.304	45
4890.406	9878	+0.297	45
4902.323	9884	+0.315	45
6080.334	10478	+0.305	27
6082.322	10479	+0.310	27
6084.303	10480	+0.308	27
6766.525	10824	+0.309	19
6774.474	10828	+0.325	19
6778.446	10830	+0.331	19
6784·410	10833	+0.345	19
6784.425	10833	+0.360	4
7018.414	10951	+0.332	20
7137.441	11011	+0.367	21
7569.7977	11029	+0.386	22
7623.332	11256	+0.374	8
7958.470	11425	+0.351	8
7958.474	11425	+0.355	5
7958.475	11425	+0.356	8
7958.477	11425	+0.358	5
8315.452	11605	+0.357	28
8321.393	11608	+0.348	28
8323.369	11609	+0.341	28
8323.413	11609	+0.385	5
8333.345	11614	+0.401	5
8670.479	11784	+0.391	2
8670.484	11784	+0.396	29
8672.430	11785	+0.359	29
8672.457	11785	+0.386	2
8680.382	11789	+0.378	2
8975.8796	11938	+0.379	12
9019.525	11960	+0.394	35
9019.526	11960	+0.395	35
9027.435	11964	+0.371	3
9027.450	11964	+0.386	5
9029.413	11965	+0.366	3
9029.439	11965	+0.392	5
9259.490	12081	+0.392	3
9259.494	12081	+0.396	24
9376.4926	12140	+0.386	6
9376.4386	12140	+0.332	6
9376.4928	12140	+0.386	11
9386.404	12145	+0.381	3
9691.8224	12299	+0.387	23
9695.7941	12301	+0.392	23
9699.7590	12303	+0.390	23
9701.7410	12304	+0.389	23
9876.268	12392	+0.395	6
9876.268	12392	+0.395	36

Continued

Table 1—*Continued*

Times of primary minima ($JD_{\odot}$)	Cycle	$O-C$	Reference
2440046.8186	12478	+0.d390	23
0443.463	12678	+0.394	30
0443.466	12678	+0.397	30
0443.471	12678	+0.402	30
0443.475	12678	+0.406	30
0443.480	12678	+0.411	30
1268.461	13094	+0.381	34
1270.435	13095	+0.372	34
1274.417	13097	+0.388	34
1506.443	13214	+0.379	33
1593.7124	13258	+0.388	7
1635.386	13279	+0.414	16
1637.344	13280	+0.389	16
1639.340	13281	+0.402	16
1639.361	13281	+0.423	16
1911.017	13418	+0.380	17
1920.948	13423	+0.395	17
1922.927	13424	+0.391	17
1936.8022	13431	+0.384	7
1938.7874	13432	+0.386	7
1962.603	13444	+0.403	37
1968.564	13447	+0.415	37
1972.536	13449	+0 420	37
1974.517	13450	+0.418	37
2285.8406	13607	+0.379	23
2287.8257	13608	+0.381	23
2287.8275	13608	+0.383	39
2289.8120	13609	+0.384	23
2319.558	13624	+0.382	17
2319.592	13624	+0.426	17
2634.8750	13783	+0.370	23
2700.3038	13816	+0.354	41
2716.1986	13824	+0.383	41
2730.0952	13831	+0.397	41

References : 1. Ahnert (1949); 2. Ahnert (1965); 3. Ahnert (1966); 4 Alexandrovich (1959); 5. Braune & Hübscher (1967); 6. Cester (1967); 7. Chambliss (1974); 8. Dueball & Lehmann (1965); 9. Dugan & Wright (1939); 10. Gainullin (1943); 11. Guarnieri *et al.* (1975); 12. Hall (1968); 13. Harper (1933); 14. Himpel (1936); 15. Ischenko (1963); 16. Isles (1973); 17. Isles (1975); 18. Jacchia (1930); 19. Karetnikov (1959); 20. Karetnikov (1961); 21. Karetnikov (1962); 22. Karle (1962); 23. Karle *et al.* (1977); 24. Kizilirmak & Pohl (1968); 25. Krat (1945); 26. Loreta (1930); 27. Makarov *et al.* (1957); 28. Oburka (1964); 29. Oburka (1965); 30. Oburka & Silhan (1970); 31. Parenago (1930); 32. Parenago (1938); 33. Peter (1972); 34. Pickup (1972); 35. Pohl & Kizilirmak (1966); 36. Pohl & Kizilirmak (1970); 37. Pokorny (1974); 38, Rügemer (1931); 39. Scarfe & Barlow (1978); 40. Schneller & Plaut (1932); 41. Srivastava (1981); 42. Svechnikov (1955); 43. Theokas (1977); 44. Wood (1946); 45. Wroblewski (1956); 46. Zverev (1936).

Table 2. Change in period and instant periods of AR Lacertae

Portion	Total change in period (days) $\times 10^{-5}$	Interval of cycles	Instant periods at points B, C, D and E (days)	Period trend
AB	4.38	E = 0 to E = 6550	1.9832438	Increase
BC	1.56	E = 6550 to E = 8650	1.9832282	Decrease
CD	4.17	E = 8650 to E = 12525	1.9832699	Increase
DE	1.79	E = 12525 to E = 13831	1.9832520	Decrease

Assuming AR Lac to be in a semi-detached state of evolution, the period changes have been interpreted on the basis of mass transfer from the secondary (cooler) component, using the model by Biermann & Hall (1973). On the assumption that the mass loss is taking place from the secondary component only and that the total angular momentum of the system remains conserved, the mass change between different portions of $O - C$ diagram is given by

$$\frac{\Delta P}{P} = -\frac{2\Delta m_2}{m_2},$$

where $m_1 \simeq m_2$.

Also, the total mass transfer between different portions of the $O - C$ diagram, *i.e.* that from A to B, B to C, C to D and D to E has been calculated on the assumption of a circular orbit, a constant mass loss from the secondary component, and using a value of $m_2 = 1.42\, M_\odot$. The extent of mass changes in different portions of $O - C$ diagram, thus calculated are given in table 3.

Table 3 indicates that the overall change in period per year is of the order of 1.7×10^{-6} d, while the average change in mass per year is of the order of $6.2 \times 10^{-7} M_\odot$. It is also evident from table 3 that the average yearly rate of period increase is slower than the average yearly rate of period decrease. Also, the average yearly rate of mass transfer in the increasing portion is lesser than the average yearly rate of mass transfer in the decreasing portion of $O - C$ diagram. This implies that the return of mass (or mass transfer) from the primary component to the secondary is slower than the rate of mass transfer from the secondary component to the primary. The short-term period changes, reflected as the scatter in the $O - C$ diagram, are also seen in the diagram.

Table 3. Mass transfer rate in AR Lacertae

Range	Yearly rate of period change (days) $\times 10^{-6}$	Yearly rate of mass change ($M_\odot$) $\times 10^{-7}$
A to B	1.22	4.36
B to C	1.42	5.07
C to D	2.09	7.45
D to E	2.24	8.01
Mean	1.74	6.22

Hall (1976) surveyed the properties of the RS CVn type binaries and mentioned that their most remarkable property is the tendency for the orbital periods to be variable. These involve both increases and decreases of the period, such that $\Delta P/P = 10^{-4}$ or 10^{-5}, the timescale being in years or tens of years.

De Campli & Baliunas (1979) computed the mass loss rates for rocket-type (or anisotropic) mass ejection, and found that the orbital period changes reported for several RS CVn systems require $dM/dt \sim 10^{-6}\, M_\odot\ \mathrm{yr}^{-1}$, and that the mass loss rate for AR Lac is of the order of $10^{-7}\, M_\odot\ \mathrm{yr}^{-1}$.

Our result, that $\Delta P \simeq 10^{-5}$ d for AR Lac, is in agreement with the surveys conducted by Hall (1976), and our derived mass transfer rate of $10^{-7}\, M_\odot\ \mathrm{yr}^{-1}$ for AR Lac is in agreement with the findings of both De Campli & Baliunas (1979), and Hall & Kreiner (1980).

Acknowledgement

The author is thankful to Dr S. D. Sinvhal for suggesting the problem and for helpful suggestions.

References

Ahnert, P. (1949) *Astr. Nachr.* **277,** 187.
Ahnert, P. (1965, 1966) *Mitt. Veränderl. Sterne* **2,** 170; **24,** 137.
Alexandrovich, Y. R. (1959) *Astr. Circ.* **205,** 19.
Arp, H. C. (1958) *Handb. Phys.* **51,** 83.
Biermann, P. & Hall, D. S. (1973) *Astr. Ap.* **27,** 249.
Braune, W. & Hübscher, J. (1967) *Astr. Nachr.* **290,** 105.
Cester, B. (1967) *Mem. Soc. Astr. Ital.* **38,** 707.
Chambliss, C. R. (1974). *I.B.V.S. No. 883.*
De Campli, W. M. & Baliunas, S. L. (1979) *Ap. J.* **230,** 815.
Dueball, J. & Lehmann, P. B. (1965) *Astr. Nachr.* **288,** 167.
Dugan R. S. & Wright, W. W. (1939) *Contr. Princeton No. 19,* 53.
Ertan, A. Y. *et al.* (1982) *Ap. Sp. Sci.* **87,** 255.
Gainullin, A. Sh. (1943) *Engelhardt. Astr. Obs. Bull.* **22,** 3.
Guarnieri, A., Bonifazi, A. & Battistini, P. (1975) *Astr. Ap. Suppl.* **20,** 199.
Hall, D. S. (1968) *I.B V.S. No. 281.*
Hall, D. S. (1976) *IAU coll. No. 29* : *Multiple Periodic Variable Stars,* Invited papers (ed. : W. S. Fitch) Reidel, p. 287.
Hall, D. S. & Kreiner, J. M. (1980) *Acta Astr.* **30,** *No. 3,* 387.
Harper, W. E. (1933) *J. R. Astr. Soc. Canada* **27,** 146.
Himpel, K. (1936) *Astr. Nachr.* **261,** 233 (6253).
Ischenko, I. M. (1963) *Trudy Tashkent Astr. Obs. Ser.* II, 9.
Isles, J. (1973, 1975) *J. Br. Astr. Assoc.* **83,** 452; **85,** 443.
Jacchia, L. (1929, 1930) *Gaz. Astr.* **16;** 19; *Astr. Nachr.* **237,** 249.
Karetnikov, V. G. (1959, 1961) *Astr. Circ.* **207,** 16; *Perem. Zvez.* **13,** 420.
Karetnikov, V G. (1962) *Astr. Circ.* **215,** 20.
Karle, J. H. (1962) *Publ. Astr. Soc. Pacific* **74, 244.**
Karle, J. H., Vaucher, Ch., Gaston, B. & Sherman, E. (1977) *Acta Astr.* **27,** 93.
Kizilirmak, A. & Pohl, E. (1968) *Astr. Nachr.* **291,** 111.
Kiziloglu, U., Derman, E., Ögelman, H. & Tokdemirf, F. (1983) *Astr. Ap.* **123, 17.**
Kopal, Z. (1955) *Ann. Ap.* **18,** 379.
Kopal, Z. (1959) *Close Binary Systems,* Chapmann & Hall, London.
Kopal, Z. (1979) *Language of the Stars,* Reidel, p. 147.
Krat, V. (1945) *Pulkovo Obs. Bull.* **16,** *No. 5, 1.*
Kurutac, M. *et al.* (1981) *Ap. Sp. Sci.* **77,** 325.
Leavitt, H., Miss. (1907) *Astr. Nachr.* **175,** 335 (4196).
Loreta, E. (1929, 1930) *Gaz. Astr.* **16,** 10; **17,** 7.
Makarov, V., Mandel, O. & Panaioti, A. (1957) *Astr. Circ.* **187,** 16.
Naftilan, S. A. & Aikman, G. C. L. (1981) *Astr. J.* **86,** *No. 5,* 766.
Naftilan, S. A. & Drake, S. A. (1977) *Ap. J.* **216,** 508.
Nha, Il-Seong & Kang, Young-Woon (1982) *Publ. Astr. Soc. Pacific.* **94,** 496.
Oburka, O. (1964, 1965) *Bull. Astr. Inst. Czech.* **15,** 250; **16,** 212.
Oburka O. & Silhan, J. (1970) *Contr. Brno.* **9,**
Paczynski, B. (1971) *A. Rev. Astr. Ap.* **9,** 183.
Parenago, P. (1930) *Astr. Nachr.* **238,** 209.
Parenago, P. (1938) *Publ. Sternberg* **13,** 35.
Peter, H. (1972) *Bedeck. Beob. Schweiz. Astr. Gesell. Bull. No. 4.*

Pickup, D. (1972) *Bedeck. Beob. Schweiz. Astr. Gesell. Bull. No. 2.*
Pohl, E. & Kizilirmak, A. (1966) *Astr. Nachr.* **289**, 191.
Pohl, E. & Kizilirmak, A. (1970) *I.B.V.S. No. 456.*

Pokorný Z. (1974) *Contr. Brno.* **17.**
Rugemer, H. (1931) *Astr. Nachr.* **245**, 37 (5859).
Russell, H. N. & Merrill, J. E. (1952) *Contr. Princeton No. 26.*
Scarfe, C. D. & Barlow, D. J. (1978) *I.B.V.S. No. 1379.*
Schneller, H. & Plant, L. (1932) *Astr. Nachr.* **254**, 387.
Srivastava, R. K. (1981) *Ap. Sp. Sci.* **78**, 123.
Srivastava, R. K. (1983) *Ph. D. Thesis*, Kumaun University, Naini Tal.
Svechnikov, M. A. (1955) *Perem. Zvez.* **10**, 262.
Theokas, A. C. (1977) *Ap. Sp. Sci.* **52**, 213.
Wood, F. B. (1946) *Contr. Princeton No. 21*, 10.
Wood, F. B., Oliver, J. P., Florkowski, D. R. & Koch, R. H. (1980) *Publ. Univ. Pennsylvania Astr. Ser.* Vol. XII, p. 310.

Wroblewski, A. (1956) *Acta Astr.* **6**, 146.
Zverev, M. (1936) *Publ. Sternberg* **8**, 43.

Bull. Astr. Soc. India (1983) 12, 61-80

Abstracts of papers presented at the ninth meeting 1983 November 22-24 at Hyderabad

The formation of ring galaxies

T. K. Chatterjee *Department of Astronomy, Osmania University, Hyderabad 500 007*

The tidal disruptive effects due to the head-on passage of a spherical galaxy through a disc galaxy have been studied at various regions of the disc galaxy and for various orientations of the disc galaxy with respect to the direction of relative motion of the two galaxies, using the impulsive approximation. The spherical galaxy is modelled as a polytrope of index $n = 4$ and the disc galaxy as an exponential disc whose surface density is given by $\sigma(r) = \sigma_c e^{-4T/R}$, where σ_c is the central density and R the radius of the disc. It is found that as a result of the collision the innermost and the outer parts of the disc galaxy are very little affected, but the intermediate region expands and gets evacuated leading to crowding of stars in a preferential region forming a ring structure. The rings are best formed for a normal on-axis collision.

The properties of the rings are determined by the dimensionless collision parameter, $r_D = (GM_S^2R_D^5)/(V^2M_DR_S^6)$, where M_S and M_D are the masses and R_S and R_D the radii of the sphere and the disc respectively, and V is the collision velocity. The case $R_S = R_D$ is investigated in detail. For the chosen models of the disc and the sphere, the rings form within the range of values of r_D given by $0.02 \lesssim r_D \lesssim 0.05$. Within this range as r_D increases the rings become sharper and their positions shift outwards with respect to the centre of the disc galaxy. A relationship exists between the position of the density maximum of the ring and r_D which enables us to find one from the other and interpret some prominent ring galaxies. The effect of introducing a bulge in the disc is to distribute the tidal disruptive effects more evenly and therefore reduce the sharpness of the ring.

Tidal effects of the galaxy on a galactic star cluster

T. Meinya Singh* *Department of Astronomy, Osmania University, Hyderabad 500 007*

Tidal force effects in binary stellar systems are studied under the simplifying assumption that the relative motion of the systems may be neglected in comparison with the stellar motions within the systems (adiabatic approximation). We apply these results to study the tidal effects of the Galaxy on a homogeneous star cluster and obtain a criterion for the stability of the cluster, which agrees well with the criterion of dynamical stability obtained by Bok (1934) and Chandrasekhar (1942). This procedure also gives a relationship between the change in the binding energy of the cluster, the density of the cluster and the critical density.

*Present address : Govt. College, Imphal.

Tidal effects in Coma cluster binary

N. Ramamani *Department of Astronomy, Osmania University, Hyderabad 500 007*

The times of merging and disruption of NGC 4874 and NGC 4889 at the centre of the Coma cluster are estimated using the adiabatic approximation (motion of the galaxies neglected compared to the motion of stars). The time of merging is 10^9 yr and the times of disruption of NGC 4874 and NGC 4889 due to their mutual tidal effects are 6×10^9 yr and 2×10^{11} yr respectively.

Changes in sizes and shapes in binary galaxies

N. Ramamani *Department of Astronomy, Osmania University, Hyderabad 500 007*

Changes in sizes and shapes of a few binaries of different mass ratios are derived numerically. In the equal-component binaries, the components experience maximum expansion, flattening and halo formation. The halo thus formed is not very extended. The energy and angular momentum gain take place through the stars in direct orbits, when they are nearest to the perturber. The retrograde orbits are found to be more stable compared to the direct orbits. Stars at the same fractional tidal radius are affected by tidal interaction to the same extent.

OCl 556—A possible double cluster

G. S. D. Babu *Indian Institute of Astrophysics, Bangalore 560 034*

Two distinct stellar concentrations separated by a small region of low star density in the direction of OCl 556 have been found from a preliminary survey with objective grating spectroscopy. The HR diagrams of both groups are superimposed on one another indicating similar distances. The possibilities of a single cluster intercepted by a foreground strip of interstellar medium or of two different clusters at the same distance are discussed.

Light curve of the RS CVn system V711 Tau = HR 1099 during 1981–82

M. B. K. Sarma, B. D. Ausekhar and B. V. N. S. Prakasa Rao
Department of Astronomy, Osmania University, Hyderabad 500 007

Observations of the RS CVn type spectroscopic binary HR 1099 (=V711 Tau) in B and V passbands for 1981–82 season are reported. Four minima, and $\varphi_{min} = 0^p.15$, $0^p.35$, $0^p.49$ and $0^p.91$ have appeared in this season. The minimum at $0^p.15$ is identified with the wave that has been appearing continuously for a long time; the minimum at $0^p.35$ is identified with the new wave that appeared during 1980.7–1981.15 and was also present in 1981.19. The two other minima seem to be newly formed ones. The original wave that has been present since 1963 seems to be migrating directly with a period of about 7.4 yr while the new wave is moving retrogradely with a period of about 4.5 yr.

Photoelectric photometry of UX Arietis

M. B. K. Sarma and B. V. N. S. Prakasa Rao *Department of Astronomy, Osmania University, Hyderabad 500 007*

Photoelectric observations of the RS CVn type non-eclipsing binary UX Arietis (G5V + KOIV, P = $6^d.4$), obtained at the Nizamiah observatory during 1975–76, 1981–82 and 1982–83 observing seasons are presented. The light curve of UX Ari showed a wave with an amplitude in *V* varying from $0^m.02$ during 1975–76 to $0^m.15$ during 1982–83. A spot cycle of period 5–6 yr is suggested. This cycle started with the wave having direct motion in the beginning and ended with retrograde motion.

An analysis of the available data shows that the light at maximum remained almost constant. It is also evident that the light curve minimum decreased with the increasing wave amplitude. The constant light at maximum, V = $6^m.51 \pm 0.03$, indicates the unspotted photospheric brightness. It is also suggested that the variation in mean *V* brightness is mainly due to spot activity and not due to intrinsic variation.

Photoelectric elements and period study of AR Lacertae

R. K. Srivastava *Uttar Pradesh State Observatory, Naini Tal 263129*

Geometrical elements of the system AR Lacertae have been obtained using Kopal's frequency-domain analysis method and compared with our earlier results obtained by Russell & Merrill's method. New elements are : $r_1 = 0.160$, $r_2 = 0.326$ and $i = 83°.5$. The absolute dimensions of the system have been derived by using the spectroscopic findings of Sanford (1951) and the new orbital elements. The revised Roche constants indicate that apparently the system is detached. However, evolutionary discussion shows that the possibility of AR Lac being in a semidetached state of evolution cannot be ruled out. The period variations have been analysed using Biermann & Hall's (1973) model in the light of mass transfer present in the system. The yearly rates of period change and mass-transfer are found to be respectively 1.7×10^{-6} d and $6.2 \times 10^{-7}\ M_\odot$.

Biermann, P. & Hall, D.S. (1973) *Astr. Ap.* **27**, 249.
Sanford, R. F. (1951) *Ap. J.* **113**, 299.

Evidence for interpulses between photometric maxima of EX Hya

D.P. Sharma, T. M. K. Marar, S. Seetha, V. N. Padmini, K. Kasturirangan and U. R. Rao *ISRO Satellite Centre, Bangalore 560 058*

J. C. Bhattacharyya and R. Rajamohan *Indian Institute of Astrophysics, Bangalore 560 034*

Light curves of EX Hya, obtained with a high speed, single channel photometer coupled to the reflector of the Kavalur observatory are presented. The observations were carried out on eight nights during 1982 and 1983 for a total duration of 13.65 hours. The data were collected mostly in white light, and occasionally in *U*, *B* and *V* bands, with integration times of 1s or 2s. Evidence for the first observation of

interpulses between the photometric maxima of EX Hya is presented. A new ephemeris for the maxima has also been derived.

Photometric observations of X Persei

B. Lokanadham, N. Rajasekhar Rao and P. Naga Prasad
Department of Astronomy, Osmania University, Hyderabad 500 007

Photometric observations of X Persei in *U*, *B*, *V* colours during 1982–83 with 48-inch telescope of the Japal-Rangapur observatory are presented. The variations in the *UBV* magnitudes of the star with its periodicity are discussed.

Spectrophotometric studies of nova Corona Austrinae 1981

B. S. Shylaja *Indian Institute of Astrophysics, Bangalore 560 034*

Spectrophotometric observation of nova Corona Austrinae 1981, during its nebular phase, are reported. The various emissions are identified. Enhanced reddening in the continuum is striking.

The peculiar features in hot Si star HD 34452

B. S. Shylaja and G. S. D. Babu *Indian Institute of Astrophysics, Bangalore 560 034*

Photoelectric spectrophotometric observations of hot Si star HD 34452 = HR 1732 obtained in the period 1979–83 are presented. The variations in certain broad band features centred around 4200, 5200, 5700 and 6300 Å, are striking and an apparent variation in the continuum itself is noticeable. The variation of the very broad feature at 5200 Å as compared to the other features is discussed in particular.

Ca II emission in Canopus

M. K. V. Bappu, M. V. Mekkaden and N. Kameswara Rao
Indian Institute of Astrophysics, Bangalore 560 034

The changes in the Ca II K line of the F0 supergiant Canopus have been studied from the high dispersion coude spectrograms obtained since 1975 with the 102-cm reflector of the Kavalur observatory. The emission in the core of the line is variable on timescales of a few days indicating transient chromospheric actviity. The nature of the variability is discussed in connection with the detection of a variable magnetic field in the star with a pseudoperiod of 22 days.

Are the changes in infrared fluxes of Mira variables (from cycle to cycle) correlated with change in their period ?

K. V. K. Iyengar *Tata Institute of Fundamental Research, Bombay 400 005*

Although it is known that light curves of Mira variables show variations from cycle to cycle, it is not known whether the flux changes from cycle to cycle are in any way

related to changes in the period of those cycles. We have analysed the *JHKL* photometric data on 13 variables in the period range 300 to 450 days to search for evidence whether the flux changes from cycle to cycle are correlated with changes in the period of those cycles (with respect to their mean period).

Optical pulsations in the cataclysmic binary 3A0729 + 103

P. C. Agrawal, K. M. V. Apparao and K. P. Singh
Tata Institute of Fundamental Research, Bombay 400 005

P. Vivekananda Rao and M. B. K. Sarma *Department of Astronomy, Osmania University, Hyderabad 500 007*

Fast photometric observations of the newly discovered cataclysmic variable 3A0729 + 103 are reported. Regular optical pulsations, with an average semi-amplitude of $\sim$ 0.15 mag in B band and having a period in agreement with that reported by McHardy *et al.* (1982), are clearly detected in the light curve of the star. The optical pulse has a sinusoidal shape. Flares with a maximum amplitude of $\sim$ 0.43 mag have also been observed. There is also suggestion of flickering on timescales of $\sim$ 10 s. It is suggested that 3A0729 + 103 is similar in character to H2252 – 035 class of cataclysmic binaries containing rapidly rotating white dwarfs. Interpretation of the period of optical pulse as the beat period leads to prediction of x-ray pulse period to be about 847 s for prograde rotation and 991 s for retrograde rotation of the white dwarf compared to the reported $\sim$ 900–1000 s period. Alternative interpretation of the observed optical pulse being due to directly beamed radiation from the vicinity of the pole of the white dwarf is also considered.

An x-ray survey of beta Cephei stars

P. C. Agrawal and K. P. Singh *Tata Institute of Fundamental Research, Bombay 400 005*

G. R. Riegler *Jet Propulsion Laboratory, California Institute of Technology, Pasadena, CA 91109, USA*

R. A. Stern *Lockheed Palo Alto Research Laboratary, Palo Alto, CA 94304, USA*

Results of an x-ray survey of beta Cephei stars carried out with the imaging proportional counter on the Einstein observatory are reported. Three of the six surveyed beta Cephei stars are detected with x-ray luminosity, L_x, lying in the range of $(0.8\text{–}4.2) \times 10^{31}$ erg s^{-1}. The mean value of the ratio of x-ray luminosity to bolometric luminosity, L_x/L_{bol}, for the beta Cephei stars, including three from an earlier survey is found to be 8.6×10^{-8}. No dependence of L_x or L_x/L_{bol} is found on the binary or short pulsation periods of the observed stars. Likewise, no correlation was found between L_x and rotation velocity of the beta Cephei stars. It is concluded that x-ray characteristics of the beta Cephei stars are indistinguishable from other B stars of similar luminosity class. There is an indication of x-ray flux variation by a factor of $\sim$ 2 on a timescale of about 10 min from β CMa. Implications of the results are briefly discussed in terms of models of x-ray emission for early type stars.

Binary modulation and transient periodic variations in x-ray emission from the AM Her binary H 0139—68

K. P. Singh and P. C. Agrawal *Tata Institute of Fundamental Research, Bombay 400 005*

G. R. Riegler *Jet Propulsion Laboratory, California Institute of Technology, Pasadena, CA 91109, USA*

We present the results of a detailed timing analysis of the soft x-ray data on the AM Her type binary H 0139 — 68, obtained with HEAO-1 and Einstein satellites. From the HEAO-1 data we demonstrate that the x-ray flux from H0139 — 68 is modulated at the 113.6363 min orbital period of its optical counterpart. The IPC data obtained with the Einstein satellite show a high and low state in the x-ray source, consistent with the binary modulation seen in the HEAO-1 data. Transient x-ray pulsations with a period of $\sim$ 275 s are observed in the IPC data during the high state. Rapid x-ray flickering is also observed in the IPC light curve and is characterized by an average *e*-folding autocorrelation time of $\sim$ 10-20 s. It is shown that the present optical and x-ray data rule out the presence of an accretion disc in the binary system. The transient pulsations could be due to periodicities induced in the accretion rate by the oscillations of magnetic flux tubes.

A new definition of effective depth of line formation in planetary atmospheres

K. D. Abhyankar and R. K. Bhatia *Department of Astronomy, Osmania University, Hyderabad 500 007*

On account of certain difficulties encountered in the use of the effective optical depth of line formation based on the generalization of Eddington-Barbier relation we have given a new definition which is obtained by modifying the weight function used by Chamberlain. It can be easily adapted for any phase function.

Rotational transitions of CO in comets

K. S. Krishnaswamy *Tata Institute of Fundamental Research, Bombay 400 005*

The rotational transition $J = 1 \rightarrow 0$ of CO at 115.3 GHz has not been detected in comets ($T_A < 0.5$ K). It is interesting, therefore, to see whether the transitions involving higher J values can be detected. With this in view, the expected intensities of various transitions for T_{ex} of 150 K and 300 K have been calculated and are given in table 1. The striking outcome of table 1 is that the intensities of lines of higher rotational quantum numbers appear to be stronger compared to those of $J = 1 \rightarrow 0$ transition.

The expected antenna temperature for $J = 1 \rightarrow 0$ transition can be calculated from the relation, $T_A \cong B\eta_B T\tau_\nu$ valid for $\tau_\nu < 1$. Here B is the beam dilution factor, η_B the beam efficiency and T the temperature of the cometary gas. For the calculation of optical depth, we have used the population in the level $V'' = 0, J'' = 0$ that has been obtained from the solution of statistical equilibrium equations based on the resonance fluorescence process. The expected antenna temperature for $J = 1 \rightarrow 0$ transition $\approx$ 0.07 K, which is consistent with the observations.

In conclusion, the lines of higher rotational transitions of CO appear to be stronger than those of $J = 1 \rightarrow 0$ transition. They might possibly give a new handle for the study of cometary coma.

Table 1. Expected intensities of rotational lines of CO for $\Delta J = 1$

J_{upper}	λ(mm)	Ratio*		J_{upper}	λ(mm)	Ratio*	
		$T = 150$ K	$T = 3000$ K			$T = 150$ K	$T = 300$ K
1	2.60	1.0	1.0	11	0.236	1.32(3)	4.39(3)
2	1.30	1.49(1)	1.54(1)	12	0.216	1.20(3)	4.98(3)
3	0.87	6.73(1)	7.38(1)	13	0.200	1.02(3)	5.39(3)
4	0.65	1.83(2)	2.17(2)	14	0.186	8.16(2)	5.60(3)
5	0.52	3.72(2)	4.82(2)	15	0.173	6.17(2)	5.59(3)
6	0.433	6.18(2)	8.95(2)	16	0.163	4.41(2)	5.38(3)
7	0.371	8.83(2)	1.46(3)	17	0.153	3.00(2)	5.00(3)
8	0.325	1.12(3)	2.14(3)	18	0.144	1.93(2)	4.51(3)
9	0.289	1.29(3)	2.90(3)	19	0.137	1.19(2)	3.93(3)
10	0.26	1.35(3)	3.68(3)	20	0.130	7.00(1)	3.34(3)

*Normalized to $J = 1 \rightarrow 0$ line.

Analysis of the profiles CO and CS in comets

K. S. Krishna Swamy *Tata Institute of Fundamental Research, Bombay 400 005*

We have calculated the synthetic profile for the $A^1\pi - X^1\Sigma^+$) bands of the molecule CO. This is based on the statistical equilibrium calculations and with resonance flourescence process as the excitation mechanism. The calculated profile is shown to compare well with the observed profile for comet West.

We have also calculated the expected profile for the (0,0) band of the molecule CS. This is shown to be in agreement with the observed profile on comet Bradfield (1979*l*).

Restriction temperature ratios in a simple three-component solar wind model

Koduvayur G. Narayana, Michael A. Heinemann and Robert L. Carovillano
Department of Physics, Boston College, Chestnut Hill, MA 02167, USA

A three-component solar wind model, with alpha particles, protons and electrons, is investigated analytically. Model assumptions include spherical symmetry, isothermal temperatures for each component, and the polarization electrostatic field as the only coupling force. We have derived conditions for the simultaneous possible critical flow speeds and critical distances. Topologies for the possible proton and alpha critical speeds are derived analytically. We have established the existence of two critical points for the three-component solar wind model. From the derived analytical expression for the critical distances at six points on the possible critical flow speed curve are obtained conditions for the allowable ranges of alpha to proton temperature ratio for the existence of a solar wind type solution. Analytical expressions for solar wind asymptotic solution are derived. Thus we have been able to show that in the three-component solar wind model there is indeed a restriction on

the allowable alpha to proton temperature ratio in order to have a smooth solar wind type solution.

Growth and separation of flare ribbons

Rajmal Jain and A. Bhatnagar *Udaipur Solar Observatory, Udaipur 313 001*

Using high resolution H-alpha observations of 30 TR-flares which occurred in spotless and spotgroup regions during phase of cycle-21 (1976–81) we made an attempt to measure area and separation of flare ribbons and flare kernels which form the ribbons. The study of the development of flare ribbons and flare kernels showed that mostly the area-curves of flare ribbons have dissimilarities. It was observed that their total areas, their peak periods and/or their rise and decay characteristics are different. Similarly, the behaviour of individual area of flare kernel was different from the kernel of opposite ribbon as well as the kernel in the same ribbon. Thus it seems that in a two-ribbon flare, each ribbon is formed by many subflares, and each behaves as an individual H-alpha flare.

The study of velocities of separation in TR-flares revealed that in many regions the flare kernels forming a ribbon do not move with the same velocity and some times a few kernels do not show any motion at all. This indicates that the velocity of separation of various parts of the ribbon is rather different. The maximum total separation velocity between two opposite kernels was found to be about 60 km s^{-1}.

Rotation and stellar evolution

S. Ramadurai *Astrophysics Group, Tata Institute of Fundamental Research, Bombay 400 005*

Paul J. Wiita *Department of Astronomy, University of Pennsylvania, Philadelphia, PA 19104, USA*

The effect of rotation on the evolution of stars of 7 and 10 $M_\odot$ has been studied using the Eggleton code for evolution. The stars with uniform rotation have been evolved from zero age main sequence to helium burning. The effects of differential rotation like mixing due to various instabilities are being incorporated. While it is found that the rotation leaves the overall evolution unaffected, the details of evolutionary characteristics are affected to a small extent.

An expression for the rate of mass loss in O and B stars

M. S. Vardya *Tata Institute of Fundamental Research, Bombay 400 005*

An expression has been derived for the rate of stellar mass loss, using dimensional analysis, physical reasoning, and mass loss rates derived from observations of O and B stars, covering a very large range in the rate of loss, luminosity, mass and radius. The normalizing constant is found to be independent of luminosity but differs for O and B type stars. Similarly, variations have been found between O, Of, O(f) and O((f)) stars.

Figures of selfgravitating homogeneous stars in different states of motion

V. K. Gurtu and D. A. Umate
Nagpur University, Nagpur

In this paper we have considered selfgravitating homogeneous stars in four states of motion *viz.* (i) static state, (ii) state of uniform rotation having angular velocity w_0, (iii) state of nonuniform rotation having angular velocity w such that $w^2 = \sum_{s=0}^{\infty} c_s (r^2 \sin^2\theta)^s$, and (iv) state of general internal motions represented by velocity $\bar{v}$ (v_r, v_θ, v_ϕ) such that $\bar{v} \times \text{curl}\ \bar{v} = \text{grad}\ Q$. Two cases, one corresponding to $v_\phi = 0$ and the other $v_\phi \neq 0$, have been considered. We have shown that they can remain in equilibrium with nearly-spherical form of freesurface.

Figures of homogeneous magnetic stars in different states of motion

V. K. Gurtu and D. A. Umate
Nagpur University, Nagpur

In this paper we have considered homogeneous magnetic stars having magnetic field $\bar{H}$ such that $\bar{H} \times \text{curl}\ \bar{H} = \text{grad}\ Q_0$ in four states of motion *viz.* (i) static state, (ii) state of uniform rotation having angular velocity w_0, (iii) state of nonuniform rotation having angular velocity w such that $w^2 = \sum_{s=0}^{\infty} c_s (r^2 \sin^2\theta)^s = f(Q_0)$, and (iv) state of general internal motion represented by velocity $\bar{v}$ such that $\bar{v} = \alpha \bar{H}$. We have shown that they can remain in equilibrium with nearly-spherical form of free-surface given by $r = a\,[1 + \sum_{n=0}^{\infty} a_n P_n (\cos\theta)]$, provided the internal magnetic field $\bar{H}$ is feeble, such that L_0^q is a small quantity of first order as a_n, where L_0 is the representative contant of $\bar{H}$ and q, a positive integer. However in those cases where the free-surface can be reduced to spherical form, $\bar{H}$ can be strong also; external magnetic field is assumed to be zero.

Effect of dustgrains on the thermal structure in a medium adjacent to H II regions

Abdul Qaiyum and S. M. Razaullah Ansari
Department of Physics, Aligarh Muslim University, Aligarh 202 001

Investigations on the importance of far-infrared radiation (FIR) field from H II region on the cooling in H I region at a low temperature are reported here. Comparisons have been made for cooling with and without FIR for abundances of atom, ion and molecule ranging between 10^{-4} to 10^{-6}. In particular, we have performed detailed calculations for cooling for temperature ranging between 10 and 100 K. It is found that FIR largely modifies the cooling at low temperature $T_e < 100$ K. The

influence of radiation field decreases as the temperature increases. For temperature $T_e > 100$ K the contribution of FIR is negligibly small. Cooling from carbon ion is more affected as compared to carbon atom. The effect of FIR field on the cooling of CO from low rotational transitions are very much affected in the presence of the radiation field. At temperature $T_e \sim 10$ K and high hydrogen density $n(H_2)$ heating instead of cooling is found to be the case because of the absorption of radiation.

Multiple scattering and the dependence of the phase variation of equivalent widths on line profile

R. K. Bhatia and K. D. Abhyankar
Department of Astronomy, Osmania University, Hyderabad 500 007

An explanation for the inverse phase effect for absorption lines formed in a Rayleigh scattering atmosphere is given in terms of multiple scattering. It is also pointed out that the inverse phase effect is a function of the line profile chosen, with the Lorentz profile giving the maximum change and the Doppler profile the least.

Variation of orbital elements in stellar triple systems

M. K. Sarma and N. B. Sanwal
Department of Astronomy, Osmania University, Hyderabad 500 007

We consider the motions in a stellar triple system as (i) the motion of a close binary member relative to its mass centre C_s and (ii) the motion of C_s relative to the centre of mass C_T of the triple system. Starting from the accelerations of the three stars relative to an inertial reference frame, we derive for both the orbits the three rectangular components R, S and W of the perturbation acceleration. Substituting these components in Gauss' equations, we obtain the osculating elements for each orbit at any time. The relations between the perturbation accelerations for different origins of reference have been derived to be applied to the observed motions in spectroscopic and visual members of triple systems.

Synchrotron radiation of high energy electrons in earth's magnetic field as a method of detecting these ultrahigh energy electrons

S. A. Stephens* and V. K. Balasubrahmanyan
NASA/Goddard Space Flight Centre, Greenbelt, Maryland, USA

With the existing techniques one can extend the measurement of high energy electrons to only about 10^{12} eV. The determination of the energy spectrum beyond this energy plays an important role in the understanding of the propagation of cosmic rays in the solar neighbourhood. When very high energy electrons enter the earth's magnetic field, they emit photons in the x- and γ-ray regions. These photons intercept the detector simultaneously and all the photons would lie along a straight

**Permanent address* : Tata Institute of Fundamental Research, Bombay 400 005.

line, because of the small emission cone. One can make use of this principle to detect ultrahigh energy electrons.

Secondary antiprotons in cosmic rays from adiabatically expanding sources

B. A. Mauger and S. A. Stephens*
NASA/Goddard Space Flight Centre, Greenbelt, Maryland, USA

High density cloudlets have been observed with densities around 10^4 cm^{-3} to 10^5 cm^{-3}. These clouds should be conducive to star formation, and eventually, supernova explosion. As the supernova expands in the dense medium, secondary antiprotons are produced. They undergo energy losses due to adiabatic expansion, collision, ionization and annihilation. Using Kahn's model for the supernova expansion, we have calculated the resultant antiproton spectrum. This spectrum is then compared with the observed flux values and we discuss some of the implications of this calculation.

Muon charge ratio, antiproton upper limit and cosmic ray propagation models

S. A. Stephens *Tata Institute of Fundamental Research, Homi Bhabha Road, Bombay 400 005*

Direct measurement of antiproton flux cannot be done with the existing techniques above a few tens of GeV. In this paper, we present an indirect method to estimate its flux using the measured muon charge ratio at sea level. It is found that the charge ratio of muons at sea level is consistent with the observed composition of cosmic rays and the characteristics of high energy interactions. By making use of the observed and calculated errors in estimating the charge ratio, upper limits to the fraction of antiprotons in cosmic rays have been obtained in the energy region between 100 and 10,000 GeV. The fraction of antiprotons in cosmic rays as a function of energy is sensitive to the type of propagation model. It is shown that one can set constraints on the extragalactic hypothesis of the observed antiprotons in the frame work of energy dependent confinement of cosmic rays in the Galaxy.

Gamma ray spectrum due to inverse compton boosting of x-rays by secondary electrons in pulsars

N. Panchapakesan and Sutapa Ranjan *Department of Physics, Delhi University, Delhi 110 007*

Charge separation takes place in the corotating magnetosphere of a pulsar where $\Omega.B = 0$. The gamma rays which are radiated by the electron accelerated in this region, collide with x-rays emitted from the pulsar surface and create secondary electron-positron pairs. Alak Ray & G. Benford have calculated the energy spectrum of these secondary electron-positron pairs. Based on their calculations is calculated the gamma ray spectrum due to inverse Compton boosting of x-rays by these secondary electrons. Implications of the results are discussed.

*Permanent address : Tata Institute of Fundamental Research, Bombay 400 005.

Magnetic pair production in Cygnus X-3 and cut-off in high energy γ-ray spectrum

S. A. Stephens and R. P. Verma *Tata Institute of Fundamental Research, Bombay 400 005*

Using extensive air shower technique, the finite flux of γ-rays of energy $> 10^{15}$ eV has been recently observed from Cygnus X-3 which exhibits 4.8 hr period modulation. The quiescent radio emission from this binary source is suggestive of the presence of strong magnetic field extending well beyond the binary orbit. We show that the high energy γ-rays traversing this magnetic field would be attenuated by magnetic pair production process, resulting in a sharp steepening of the spectrum beyond about 10^{16} eV. Using the observed spectral steepening, we conclude that the strength of the magnetic field at $\sim 10^{14}$ cm from the source, where most of the radio emission comes from, is about 0.5 Gauss. We predict that the relative contribution of the steady γ-ray flux would increase beyond 10^{16} eV. We also discuss some of the effects of the magnetic field surrounding the companion star on the spectral shape of low energy γ-rays and on the asymmetry of γ-ray peaks in the phase diagram about the x-ray minimum.

IPS observations of an unbiased sample of Ooty occultation radio sources at 326.5 MHz

D. G. Banhatti and S. Ananthakrishnan
Radio Astronomy Centre (TIFR), Post Box 8, Ootacamund 643 001

An unbiased sample of 90 radio sources selected from the ninth Ooty lunar occultation list which are stronger than 0.75 Jy at 91.8 cm and outside the Galactic plane has been studied with the interplanetary scintillation (IPS) method. We report the results for 48 of these sources (median flux density 1.2 Jy) for which the analysis is complete. On an average 22.5% of the emission from the sources comes from a region of angular size of about 0.3 arcsec. Breaking the sample into three ranges of largest angular size (LAS) shows that the scintillating component weakens and broadens with increasing LAS. A log-log plot of the median scintillating size against the median LAS for these three classes shows an approximately linear relation with a slope of about 0.2. This relation is reinforced by the median values of scintillating size and LAS of another independent sample of sources having LAS values in the smallest LAS range here. If the scintillating structure is interpreted as due to hot spots at the ends of relativistic jets which power double radio sources, this very small slope indicates that the jets do not expand freely throughout their length (for which case the slope would be unity), but are confined at least during a substantial part of the passage from the central engine to the outer lobes.

Collimation of extragalactic jets : evidence from hot spots

D. G. Banhatti *Radio Astronomy Centre (TIFR), Post Box 8, Ootacamund 643 001*

Two pieces of evidence bearing on the collimation of extragalactic jets are presented. (i) Metre wavelength IPS observations give the overall angular size ψ of scintillating

compact structure. From 92-cm IPS data on a sample of weak radio sources, log ψ *vs* log LAS is seen on an average to have a slope much less than one. The same trend is seen from 81.5 MHz IPS data on a sample of strong sources. If ψ represents the hot spot size, this indicates that the jets giving rise to hot spots at their ends do not expand freely throughout their length. For a freely expanding jet, the expected slope is unity. (ii) A linear relation with slope near unity is found between the logarithms of the hot spot size perpendicular to the source major axis ψ_{HS} and the distance from the core θ for the 14 compact and/or intense hot spots selected from a sample of 31 quasars of the largest angular sizes observed at 4.87 GHz with subarcsec resolution. The intercept for this relation implies a (free) jet opening angle of about 1 deg if the jet is stable. For a confined jet, if it jitters (or precesses fast) in an axisymmetric way, we get an intrinsic jet opening angle of about 0.1 deg for a semiangle of 'jitter cone' (or precession cone) of 15 to 20 deg. The small slope and large scatter in the relations derived from the IPS data are probably due to (a) projection effects and (b) because the IPS method averages over all compact structure present in the telescope beam.

Extragalactic radio sources with asymmetric structure

D. J. Saikia and P. Shastri *Radio Astronomy Centre (TIFR), Post Box 1234, Bangalore 560 012*

R. P. Sinha *Systems and Applied Science Corporation, 5809 Annapolis Road, Hyattsville, MD 20784, USA*

V. K. Kapahi *Radio Astronomy Centre (TIFR), Post Box 1234, Bangalore 560 012*

G. Swarup *Radio Astronomy Centre (TIFR), P. O. Box 8, Ootacamund 643 001*

We present results of high resolution observations of $\sim$ 30 sources which were earlier classified to have extended radio emission only on one side of the compact nuclear component. Almost all these sources are identified with quasars. About 25% of them still appear one-sided whereas a majority of the rest are triple with extended emission on both sides of the nucleus. However, many of them are very asymmetric either in location or surface brightness of the outer components. Three of them appear as compact, unresolved sources in these observations. We have combined our data with other quasars whose structures are available in the literature to examine several simple predictions of the relativistic beaming hypothesis. We find the data to be broadly consistent with this scenario.

High resolution observations of nearby galaxies

D. J. Saikia[1], T. J. Cornwell[2] and V. K. Kapahi[1]
[1]*Radio Astronomy Centre, TIFR, Post Box 1234, Bangalore 560 012*
[2]*National Radio Astronomy Observatory, VLA Program, Socorro, NM 87801, USA*

It has been pointed out by Kapahi & Saikia (1982) that the radio axis defined by the outer lobes appears reasonably well aligned with the minor axis of the parent galaxy for sources with prominent cores, while those with weak cores do not exhibit a preference towards any particular axis. To investigate possible explanations for this relationship we have observed a sample of nearby galaxies with the highest

resolutions at the VLA. We have re-examined this relationship using the new data and find it to be highly significant. If this correlation is due to thermal absorption by ionized gas that is distributed differently in the two groups, one might expect a difference in their core spectra. Our observations, however, do not appear to indicate any such trend.

Many of the sources in our sample exhibit interesting radio jets. We present maps of a few of them and discuss their possible implications.

Kapahi, V. K. & Saikia, D. J. (1982) *J. Ap. Astr.* **3**, 161.

Radio continuum observations of near by galaxies

S. Sukumar *Radio Astronomy Centre (TIFR), P. B. No. 8, Ootacamund 643 001*

We have undertaken an observational study of radio continuum emission from near by galaxies. The aim of the study is to (i) unambiguously separate the thermal and nonthermal emission in the disc, (ii) study the synchrotron emission as a function of z distance from the plane of the galaxy, and (iii) derive detailed models for the origin and propagation of relativistic electrons in the disc and halo of normal galaxies.

We present preliminary radio maps at 327 MHz of two near by galaxies (NGC 4631 and NGC 1316) made with the partially operational Ooty synthesis radio telescope. The maps have a resolution of $\sim 60'' \times 120''$. A jet-like feature in NGC 1316 and the radio extent of NGC 4631 in the z-direction are discussed.

Quasars with radio jets

D. J. Saikia *Radio Astronomy Centre (TIFR), Post Box 1234, Bangalore 560 012*

If the observed asymmetry in the radio jets is due to relativistic beaming, then the approaching outer component can be identified and this should always appear further from the core than the receding one in an intrinsically symmetric, collinear source. We, however, find from a sample of quasars observed with high angular resolution that this component tends to be nearer the core in about half the cases. We investigate possible explanations for such an effect and suggest that intrinsic noncollinearity and the existence of extremely dissipative and asymmetric beams probably play an important role.

A relation between the core polarization at λ6 cm and the overall radio axes of quasars

D. J. Saikia and P. Shastri *Radio Astronomy Centre (TIFR), Post Box 1234, Bangalore 560012*

For a sample of $\sim$ 180 quasars observed with high angular resolution at the VLA, we have investigated the relative orientation of the core polarization vector at λ6 cm and the overall radio axis. In the well-observed double sources with lobes of radio emission on both sides of the nucleus, there is a strong tendency for the polarization vcetor to be perpendicular to the radio axis. Sources with a single detected

secondary component also exhibit a similar trend but at a much reduced level of significance. The latter group of sources usually tends to have very prominent cores.

Assuming Faraday rotation to be small at this frequency, the direction of the core magnetic field, which presumably is the direction of the nuclear VLBI-scale jets, can be inferred from the polarization axis. The alignment of the core magnetic field with the radio axis in triples indicates a stable long-term memory of the nuclear ejection axis. The weaker trend for sources with single secondaries and strong cores may be interpreted as due to amplification of projection effects in sources inclined at small angles to the line of sight. These results are consistent with earlier VLBI studies of the nuclear regions of a handful of sources.

Radio detection of a 'jet' in the Crab nebula

T. Velusamy *Radio Astronomy Centre (TIFR), P. O. Box 8, Ootacamund 643 001*

A recent optical picture of the 'jet' in the Crab nebula shows a tubular structure with strikingly well-collimated sharp parallel boundaries. The angular size of the jet is $75'' \times 45''$. In this paper we report the first detection of radio emission at 20 cm from this jet in the VLA map of the Crab nebula obtained with resolution of $15'' \times 15''$ and high dynamic range of about 1000. Although the jet is not fully resolved in the VLA map, its positional coincidence and structural similarity to the optical jet are remarkable. The radio emission is of extremely low surface brightness ($< 1\%$ of the surface brightness within the nebula). The radio emission appears to be nonthermal as indicated by the strong polarization ($\sim 30\%$) near its base closer to the nebular boundary. The origin of this unique feature in the Crab nebula is very puzzling, as it may be related to the supernova remnant shell, the Crab pulsar, SN 1054, or to the progenitor of SN 1054. Interpretations of the radio emission in terms of plasma instabilities within the remnant or Rayleigh-Taylor instability of a relativistic cavity pushing against interstellar medium are examined.

Narrow-band, short duration radio bursts at decameter wavelengths and their interpretation

N. Gopalswamy, G. Thejappa, K. R. Subramanian and Ch. V. Sastry
Indian Institute of Astrophysics, Bangalore 560034 and Raman Research Institute, Bangalore 560080

Narrow-band, short-duration radio bursts observed at 34.5 MHz are reported Main observational features are : (i) single frequency duration, $\Delta t \sim 300$ ms; (ii) relative bandwidth $\Delta f/f \sim 3\%$; and (iii) frequency drift ~ 250 kHz s^{-1}. These characteristics show that the bursts are of type I(d). Emerging flux theory of type I bursts proposed by Spicer *et al.* (1981) is modified to explain the observations. Whereas they invoke the coalescence of upper hybrid (UH) waves with the shock-generated lower hybrid (LH) waves as the radiation mechanism, we show that the coalescence of the UH waves with perpendicular ion-sound (IS) waves is more favourable. The saturation energy density of the IS waves is two orders of magnitude larger than that of the LH waves. Moreover, the overlapping in K-space is

more in the case of IS waves as compared to LH waves. We have also estimated the coronal magnetic field, using the observed bandwidth, the observed drift velocity in the Rankine-Hugoniot relation for perpendicular shock waves. The value is $\sim$ 1 Gauss which is in good agreement with other estimates like frequency splitting and polarization measurements of type I bursts.

Spicer, D. S., Benz, A. O. & Huba, J. D. (1981) *Astr Ap.* **105**, 221.

Hard x-ray spectrum of solar burst of 1980 June 4

B. Lokanadham and P. K. Subramaniam
Department of Astronomy, Osmania University, Hyderabad 500 007

Alan L. Kiplinger and B. R. Dennis *Goddard Space Flight Centre, Greenbelt, Maryland, USA*

This paper presents a study of the x-ray spectrum of a solar burst recorded by the hard x-ray burst spectrometer on SMM satellite on 1980 June 4, at 0830 U.T. The hard x-ray time-profile is characterized by an initial pulse train of intense hard x-ray spikes. The energy spectrum in 28–125 keV energy band is represented by a power law with an exponent of $\sim$ 3.7. Studies of the temporal and spectral properties of the event indicate that the sequential firing loop mechanism is responsible for the observed flare. This event has also been recorded simultaneously on the ground by the microwave solar radiometers in 1–20 GHz frequency range.

A study of quiet sun radiation at cm wavelengths during solar maximum period 1980–81

B. Lokanadham and P. K. Subramanian
Department of Astronomy, Osmania University, Hyderabad 500 007

Observations of solar radio emission at 3 cm wavelength have been made at Japal-Rangapur observatory for 1980–81, the solar maximum year, using the 3-m radio telescope. The correlation between microwave solar emission and the sunspot activity has been found to be high during the maximum phase and in the high cm wavelength band. The basic component has been estimated statistically for successive solar rotations using the data obtained at Japal-Rangapur observatory. Further, this was compared with the data obtained at other cm wavelengths in 1980–81 and the solar minimum period 1975–76 of the 21st cycle. The computed values showed pronounced variation at high cm wavelengths for the solar maximum period with dissimilar variations at different wavelengths. During the solar minimum period the variations are negligibly small and showed more or less constant level of activity.

Implications of escape of supermassive blackholes from galactic nuclei due to plasmoid ejection

R. C. Kapoor *Indian Institute of Astrophysics, Bangalore 560 034*

Shklovsky (1982: *IAU Symp. No. 97*, p. 475) has hypothesized escape of accreting supermassive blackholes from galactic nuclei as a consequence of asymmetric ejection of

plasma clouds from their accretion discs and their subsequent defunction for explaining evolutionary effects in quasars. It is argued here that such an interpretation must accommodate the possibility of substantial capture of stars and gas by the blackhole on its way out—which can prolong the life of the quasar—unless the mass of the blackhole is less than $10^7 M_\odot$ and a large enough initial recoil velocity is achieved.

Behaviour of scalar particles near a Schwarzschild blackhole

S. Banerji and T. K. Das *Department of Physics, University of Burdwan, Burdwan 713 104*

D. R. Mandal *Department of Physics, Basirhat College, Basirhat, West Bengal*

In a previous paper Banerji & Mandal set up the Klein-Gordon equation in the background of the Schwarzschild curved spacetime and showed that bound state solutions exist for particles of energy less than the rest energy. They, however, considered only radial particles ($l = 0$) and neglected an attractive r^{-4} term. Here we get rid of the above two assumptions and show that the bound states still exist with a certain decay constant for energy of the particles smaller than the rest energy. For energies greater than the rest energy the particles are partly scattered and partly absorbed.

Gamma rays from rotating blackholes

N. Panchapakesan and Vijoy Prakash *Department of Physics, University of Delhi, Delhi*

The gamma ray luminosity due to the decay of pions produced during spherical accretion onto a rotating blackhole has been calculated. The model consists of a Kerr blackhole of arbitrary angular momentum surrounded by interstellar gas consisting of completely ionized hydrogen atoms. As protons are accelerated in the accretion disc of blackhole the process $p + p \ldots\ldots p + p + \pi^\circ$, $\pi^\circ \rightarrow 2\gamma$ produces gamma rays. Using a N* model the flux can be calculated from known production cross-sections and their temperature dependance. To decide which of these photons are able to come out one has to use knowledge of the properties of orbits of massless particles in Kerr metric. There is an 80% increase in flux as we go from Schwarzschild to the extreme Kerr case.

Radiating viscous fluid spheres in general relativity

K. S. Bhamra *Mathematics Department, Manipur University, Imphal 795 003*

K. Manihar Singh *Mathematics Department, Oriental College, Imphal*

We study the time-dependent field equations for radiating viscous fluid spheres, where we take the energy-momentum tensor as the sum of the energy-momentum tensor for a viscous fluid and a radially expanding radiation. We present some new exact analytic solutions with the corresponding pressure, density and luminosity distributions. We also present a case by choosing one of the metric elements such that distribution of physical quantities is reasonable. The solutions we have considered represent viscous fluid spheres in equilibrium.

A cluster of galaxies in time-varying gravity sense

Neeraj Chaubey *Department of Applied Sciences, Kamla Nehru Institute of Technology, Sultanpur (Avadh) 228 001, UP*

We present a classical mechanical model of a cluster of galaxies under the Hubble constraint in a Newtonian frame wherein the constant of gravitation depends on time.

[Fe XIV] 5303 Å emission line profiles of the total solar eclipse of 1983 June 11

Jagdev Singh and K. R. Sivaraman *Indian Institute of Astrophysics, Bangalore 560 034*

Spectra of the solar corona in the [Fe XIV] 5303 Å line were obtained using a high resolution multislit spectrograph during the 1983 total solar eclipse at Java. The spectrograph was designed to provide a dispersion of 2.2 Å mm^{-1}. The line widths measured from 1.040 to 1.245 $R_\odot$ with a spatial resolution of $6'' \times 9''$ vary from 0.6 Å to 1.4 Å with a peak at 0.9 Å. This peak value corresponds to a temperature of 3.1×10^6 K. If temperatures of the order of 2.3×10^6 K are typical of the regions that emit 5303 Å radiation then microturbulent velocities of the order of 16 km s^{-1} will have to be invoked to explain the enhanced line broadening.

The value of the microturbulent velocity obtained at the solar eclipse of 1980, which was a solar maximum year, was 30 km s^{-1}. It would thus seem that microturbulence is a function of solar activity, increasing when the activity increases.

The scanning spectrometer of the Japal-Rangapur observatory

R. Swaminathan *Department of Astronomy, Osmania University, Hyderabad 500 007*

A single-channel Czerny-Turner type scanning spectrometer has been fabricated and is being successfully used at the Nasmyth focus of the 1.22-m telescope of the Japal-Rangapur observatory.

The instrument consists of a collimator and camera mirrors of 1-m focal length, a 600 gr mm^{-1} grating blazed at λ7500 Å in the I order, an entrance diaphragm wheel and an exit slot, apart from a filter slide to sort out the overlapping orders. At the exit slot end is a photomultiplier cold box with provision to cool the tube to dry-ice temperatures. An EMI 9502 B (S-11) photomultiplier tube in the spectral range λ2600–5400 Å is currently being used. The scanner has a reciprocal linear dispersion of 8 Å mm^{-1} in the II order blue and gives a spectral purity of approximately 1.6 Å for a 2.5 arcsec seeing disc of the star.

The system is being used in an analogue mode, with a DC amplifier and strip-chart recorder. A photon-counting circuitry is being completed now. The instrument will then be used as a rapid scanner and the data logged by a microprocessor-based data acquisition system. The data logger is capable of collecting information over 2000 channels or 1000 each in the forward (increasing wavelength) and reverse directions, averaging the signal over a total of up to 99 scans for a better signal-to-noise ratio. In each channel which could be preselected it can integrate from 1 ms to 99 s. A control for the stepper motor for rotating the grating through a sine-bar mechanism is incorporated.

Design of an echelle spectrograph for the Japal-Rangapur observatory

R. K. Bhatia, R. Swaminathan and M. L. Vyas
Department of Astronomy, Osmania University, Hyderabad 500 007

The design considerations of a high dispersion echelle spectrograph for use at the Nasmyth focus of the 1.22-m telescope of the Japal-Rangapur observatory are presented. An interesting feature of the design consists in using a post-dispersion dichroic filter to facilitate simultaneous recording of the spectra in both the blue and red regions, using different imaging systems.

On the efficiency of existing spectrographs at higher dispersions

R. K. Bhatia and N. Ramamani *Department of Astronomy, Osmania University, Hyderabad 500 007*

The efficiency of existing spectrographs at higher dispersions has been examined. It is concluded that in most cases a simple change of grating, while giving higher dispersion, can lead to light losses which become serious with increasing dispersion.

A high time resolution gamma ray burst payload for photometry and spectroscopy

T. M. K. Marar, D. P. Sharma, Sreenivasaiah, K. V. S. Seetha, B. V. Nagaraja, V. P. Dewangan, K. Kasturirangan and U. R. Rao
ISRO Satellite Centre, Bangalore 560 058

An experiment designed to monitor and study celestial gamma ray bursts in the energy range 20 keV–3 MeV is described. The experiment employing two CsI(Na) scintillators of 45.6 cm^2 and 11.3 cm^2 area for the detection of gamma rays will be launched onboard the first mission of the 150 kg class of stretched Rohini series of satellites during 1985. It has unique capabilities of detecting and measuring bursts to a 3 sigma sensitivity level of about 5×10^{-6} erg cm^{-2}. Very high temporal resolutions of 2 ms and 16 ms are available during the peak of the burst up to 8 s and 1 s prior to burst detection. The temporal evolution of the bursts can be studied for a total duration of 204 s after burst detection. The experiment therefore has the capability to study both short and long duration bursts. Temporal evolution of the bursts spectra can be studied for a duration of 16 s after and 2 s before the burst trigger. Spectral and temporal informations on the precursors will therefore be available for the first time in the study of gamma ray bursts. The high time resolution photometric and spectroscopic capabilities of the experiment in the above time frame are expected to shed more light on the origin and production mechanisms of gamma ray bursts.

A new polarimeter for emission corona

A. J. Kamatgi, D. B. Jadhav and A. D. Tillu
Department of Physics, University of Poona, Pune 411 007

The coronal 5303Å emission was directly detected against photospheric background in 1980, using the then recently developed spectral scanning polarimeter with a

resolution of 4 Å. These measurements were repeated and confirmed in 1983 by using an improved set-up having a resolution of 0.4 Å, and besides 5303 Å, 6374 Å coronal line was also detected. Since the instrument has been mainly designed for day glow emission studies, number of inherent obstacles exist for routine monitoring of coronal emission lines and the following new system for simultaneous measurements of polarization and intensities of coronal emission lines is proposed to be built. It will consist of the following functional units : (i) twin channel imaging system, (ii) twin channel polarization unit, (iii) half-meter Czerny-Turner monochromator (CTM) and (iv) microprocessor based data acquisition system.

Latest results of the Danjon astrolabe observatory

M. G. Arur, P. S. Bains and Santokh Singh
Survey of India,Geodetic and Research Branch, Post Box 77, Dehra Dun 248 001

Danjon astrolabe, fitted in the compound of geodetic and research branch of Survey of India, is briefly described. The utility of its data is mentioned and latest results of astronomical observations presented.